Elastic scattering of slow electrons by *n*-propanol and *n*-butanol

M. A. Khakoo,[1] J. Muse,[1] H. Silva,[2] M. C. A. Lopes,[2] C. Winstead,[3] V. McKoy,[3] E. M. de Oliveira,[4] R. F. da Costa,[4] M. T. do N. Varella,[5] M. H. F. Bettega,[6] and M. A. P. Lima[4,7]

[1]*Department of Physics, California State University, Fullerton, California 92834, USA*
[2]*Departamento de Física, ICE, Universidade Federal de Juiz de Fora, Juiz de Fora-MG, CEP 36036-330, Brazil*
[3]*A. A. Noyes Laboratory of Chemical Physics, California Institute of Technology, Pasadena, California 91125, USA*
[4]*Instituto de Física Gleb Wataghin, Universidade Estadual de Campinas, Caixa Postal 6165, 13083-970, Campinas, São Paulo, Brazil*
[5]*Centro de Ciências Naturais e Humanas, Universidade Federal do ABC, Rua Santa Adélia, 166, 09210-170, Santo André, São Paulo, Brazil*
[6]*Departamento de Física, Universidade Federal do Paraná, Caixa Postal 19044, 81531-990, Curitiba, Paraná, Brazil*
[7]*Centro de Ciência e Tecnologia do Bioetanol CTBE, Caixa Postal 6170, 13083-970, Campinas, São Paulo, Brazil*

We report measured and calculated cross sections for elastic scattering of low-energy electrons by the alcohols *n*-propanol and *n*-butanol in the gas phase. The measurements were carried out using the relative-flow method with an aperture source rather than a conventional tube or capillary-array source, eliminating the need to know molecular diameters. The calculations employed two different implementations of the Schwinger multichannel variational method and included polarization effects. The differential cross sections are dominated by strong forward scattering due to the molecules' large electric dipole moments, but near 10 eV, they display structure at intermediate angles that is probably associated with shape resonances, notably a pronounced *f*-wave scattering pattern. Overall agreement between the measured and calculated results is fair. We compare the cross sections of these larger alcohols to those of methanol and ethanol, as well as to those of alkanes.

I. INTRODUCTION

Increased interest in electron-driven processes involving biomolecules has prompted several recent studies of collisions between slow electrons and alcohols [1–6]. In developing a detailed understanding of radiation damage to living systems induced by secondary electrons, alcohols may serve as analogs for the subunits of large biomolecules. Moreover, electron collisions are relevant to spark ignition and combustion of alcohols used as biofuels. To date, electron interactions with the two smallest alcohols, methanol (CH_3OH) and ethanol (C_2H_5OH), have received the most attention; however, larger alcohols are also of interest. In particular, butanol (C_4H_9OH), which can be produced by bacterial fermentation of lignocellulosic biomass, has attracted attention as a potential biofuel [7].

Here we report results from a combined experimental and computational study of low-energy elastic electron scattering by the straight-chain, primary isomers of propanol (C_3H_7OH) and butanol, *n*-propanol and *n*-butanol (also known as 1-propanol and 1-butanol or propan-1-ol and butan-1-ol). For both molecules, we measured absolute differential elastic cross sections at selected energies from 1 to 100 eV using a recently developed modification of the relative-flow technique [8]. We carried out corresponding cross-section calculations in the fixed-nuclei, static-exchange plus polarization (SEP) approximation using two different implementations [9,10] of the Schwinger multichannel method [11,12], with corrections for long-range scattering by the dipole potential included through the point-dipole Born approximation [6].

The present measurements and calculations of electron cross sections for *n*-propanol and *n*-butanol extend our ear-

lier work on methanol and ethanol [6]. Although electron-impact ionization cross sections have previously been measured for *n*-propanol [13–15] and *n*-butanol [15,16], to our knowledge, no prior elastic-scattering data, experimental or theoretical, exist for either molecule.

II. METHOD

A. Experiment

The present apparatus and experimental procedure have been detailed in Ref. [6] and references therein. Hence only a brief description will be given here. The relative-flow method with a collimating thin-aperture source was used in this work, as in Ref. [6], with He as the standard gas. The spectrometer used cylindrical electrostatic optics and double hemispherical energy selectors in both the electron gun and the detector. Energy loss spectra of the elastic peak were collected at fixed values of the incident electron energy E_0 and scattering angle θ by repetitive, multichannel scaling techniques. The target gas beam was formed by effusing the gas through a thin aperture [6]. The target source and the spectrometer surfaces around the collision region were heavily sooted to reduce secondary electrons. This source was incorporated into a movable-source [17] arrangement. In this method, the gas-collimating structure is moved into (signal+background) and out of (background) the collision region center (see Ref. [6] for details). We calibrated the spectrometer contact potential from the $1s2s^2(^2S)$ resonance in He at the incident energy of 19.366 eV [18] to within an estimated ± 0.04 eV repeatedly during the course of the experiment to check the stability of the electron beam. Typical

currents for the electron beam ranged around 20–25 nA, with a resolution of 60 meV (full width at half maximum).

We operated our experiment at low pressures, typically <2 Torr for He, <0.15 Torr for *n*-propanol, and <0.1 Torr for *n*-butanol, which are well below the pressures corresponding to the critical mean free path (i.e., that equal to the aperture thickness of 0.025 mm) for these gases (5 Torr for He, ≈0.44 Torr for *n*-propanol, and ≈0.2 Torr for *n*-butanol, using molecular diameters of 7.5×10^{-8} cm and 8.2×10^{-8} cm for *n*-propanol and *n*-butanol, respectively, obtained from our gas flow analysis [6]). ACS-grade liquids (quoted purity of 99.9%) were used to produce the target gases. The gas lines were operated at 347 K to prevent condensation in the gas lines, while the spectrometer was operated at 393 K to ensure that the gases did not condense on the instrument, thus providing stability of the electron spectrometer operation during the experiment to better than 10%. The experimental chamber typically remained in the pressure range of $(0.7–1.5) \times 10^{-6}$ Torr for the drive pressures used in this work, and the incident electron current remained stable within 10% or better, even when different gases were flowed.

The spectrometer acquisition was mostly computer controlled. The computer located the scattering angle and scanned the elastic scattering spectra, storing these along with the gas drive pressure (taken for each scan) as measured by the Baratron manometer. The gas drive pressure was used to determine the gas relative-flow rate [6]. The relative incident electron current was determined using a sooted molybdenum beam flag placed in front of the electron beam with an approximately 35-V bias to collect the electrons. The flag was used during every interval when the spectrometer was moved from one angle to the next, then moved out of place and its voltage set to ground (collision region potential). The gas whose cross section was to be determined was flowed following He, and scattered count rates for a range of angles were obtained. This process was repeated to check for reproducibility. The differential cross section (DCS) for *n*-propanol or *n*-butanol, $\mathcal{Q}_X(E_0, \theta)$, is obtained from the relative-flow equation [6]

$$\mathcal{Q}_X(E_0, \theta) = \mathcal{Q}_{\text{He}}(E_0, \theta) \frac{\mathcal{R}_{\text{He}} I_{s,X}}{\mathcal{R}_X I_{s,\text{He}}} \sqrt{\frac{M_{\text{He}}}{M_X}}, \qquad (1)$$

where I_s are the background-corrected scattering rates, $\mathcal{R}$ the relative-flow rates (RFRs), and M the molar masses, and where subscripts X and He indicate the gases concerned, X being either propanol or butanol. The He elastic DCSs were taken from Refs. [19,20].

Using the apparatus and procedure described, we determined elastic electron-scattering cross sections for *n*-propanol and *n*-butanol at E_0 values of 1, 2, 5, 10, 15, 20, 30, 50, and 100 eV for scattering angles from 5° to 130°, over a coarser interval (20°) at large scattering angles than at small scattering angles (10°).

B. Computational

The all-electron SMC calculations employed nuclear geometries for *n*-propanol and *n*-butanol that were optimized at the level of second-order Möller-Plesset perturbation theory using the electronic structure package GAMESS [21] and the 6-31G(*d*) basis set as contained therein. For both molecules, we assumed all-*trans* conformations having C_s point-group symmetry. The presence of symmetry facilitates the evaluation of cross sections by allowing us to carry out separate scattering calculations for the $^2A'$ and $^2A''$ representations of C_s. Experiments and calculations [22–24] indicate that the lowest-energy conformers of both *n*-propanol and *n*-butanol in the gas phase are in fact C_1 structures with the OH group *gauche* to the plane of the carbon atoms. However, the energy splittings are small, and several conformers, including all-*trans*, will be present at room temperature. We have not attempted to take the possible effects of such variations in nuclear geometry into account, and thus have implicitly assumed them to be small. The target electron density was obtained at the restricted Hartree-Fock level in the "double-zeta valence" (DZV) basis set as defined in GAMESS with a $2d1s1p$ diffuse and polarization supplement on C and O atoms and a $1s1p$ supplement on H atoms, using GAMESS's default exponents and splitting factors for the supplemental functions and excluding the $x^2+y^2+z^2$ linear combination of Cartesian d orbitals.

The variational trial space for describing the electron-molecule scattering system contained all antisymmetrized products of the Hartree-Fock ground state of the target molecule with one of the virtual orbitals as well as spin-adapted (doublet) products of singlet singly excited configurations of the target with a virtual orbital, the latter included to describe polarization effects—i.e., target relaxation during the collision. To accelerate convergence of the polarization space, the Hartree-Fock virtual orbitals were first transformed into modified virtual orbitals (MVOs) [26] calculated in the field of a closed-shell cationic Fock operator with charge 6+. For propanol, we included excitations from the 9 outermost occupied valence orbitals into the 20 lowest-energy MVOs when forming the polarization space; for butanol, we included excitations from the 10 outermost valence orbitals into the 20 lowest MVOs. The resulting variational spaces comprised 10 423 A' and 10 130 A'' configuration-state functions (CSFs) for propanol and 14 548 A' and 14 506 A'' CSFs for butanol.

In the calculations that employed the Schwinger multichannel method with pseudopotentials [10], the basis sets used to describe bound and scattering states include $5s5p3d$ uncontracted Cartesian Gaussian functions on the carbon and oxygen atoms, generated as described in Ref. [27] and listed in Table I. For the hydrogen atoms, we used the $4s/3s1p$ basis of Dunning [28]. The pseudopotentials of Bachelet, Hamann, and Schlüter [29] were used to replace the core electrons of the carbon and oxygen atoms. The propanol nuclear geometry was optimized using GAMESS [21] at the Hartree-Fock level within the 6-311G($2d, 1p$) basis set. For butanol, we used the same geometry as in the all-electron calculations described above. The computed values for the dipole moment, 1.58 D for propanol and 1.72 D for butanol, agree fairly well with the respective experimental values of 1.55 and 1.66 D [25]; the target states used in the all-electron calculation give somewhat larger values, 1.69 and 1.75 D, respectively.

TABLE I. Uncontracted Cartesian Gaussian functions used for carbon and oxygen.

Type	Carbon Exponent	Oxygen Exponent
s	12.49628	16.05878
s	2.470286	5.920242
s	0.614028	1.034907
s	0.184028	0.316843
s	0.039982	0.065203
p	5.228869	10.14127
p	1.592058	2.783023
p	0.568612	0.841010
p	0.210326	0.232940
p	0.072250	0.052211
d	1.794795	1.698024
d	0.420257	0.455259
d	0.101114	0.146894

As in the all-electron calculations, polarization effects were included by considering single excitations from the valence occupied orbitals to a set of MVOs [26]. As mentioned above and described elsewhere [30], MVOs provide efficient representations of particle and scattering orbitals when describing polarization effects. For both propanol and butanol, we generated the MVOs by diagonalizing a Fock operator for a cation of charge 2+. For propanol, we considered excitations to MVOs with eigenvalues less than 4 eV. These orbitals were also used as scattering orbitals. We included singlet- and triplet-coupled excitations, giving 6057 CSFs for A' symmetry and 5794 CSFs for A'' symmetry. For butanol, we considered excitations to orbitals with eigenvalues less than 5 eV and used the same set of orbitals as scattering orbitals. Considering singlet- and triplet-coupled excitations, we obtained for butanol 8998 CSFs of A' and 8660 of A'' symmetry. The total number of CSFs used in the expansion of the scattering wave function was thus 11 851 for propanol and 17 658 for butanol.

Because the variational spaces used in the SMC calculations are built from short-range, square-integrable functions, the scattering amplitudes we obtain describe scattering by the short-range part of the electron-molecule potential, but do not account well for scattering by the $\sim r^{-2}$ potential associated with the substantial electric dipole moments of n-propanol and n-butanol. This long-range potential weakly scatters electrons even at large impact parameters, producing a strong forward peak in the differential cross section. To incorporate the dipole-scattering contribution, we employ closure procedures that combine the SMC scattering amplitudes with the first Born approximation to the scattering amplitude of a point dipole. The same procedures were used as in earlier work on methanol and ethanol [6], with the difference that, in the all-electron work, a sign error in the dipole amplitude has been corrected; this error caused oscillations in the methanol and ethanol differential cross sections over the $\sim 20°-50°$ angular range at 5 eV and below. Smooth

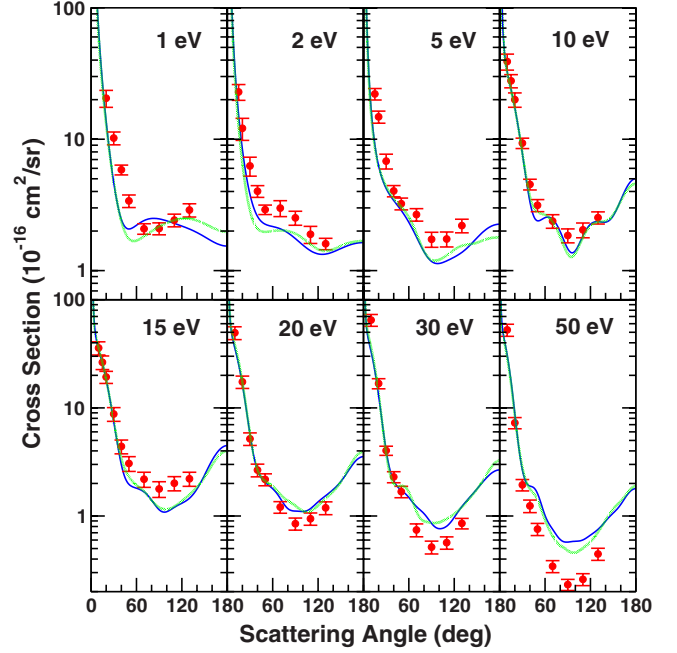

FIG. 1. (Color online) Differential cross sections for elastic scattering of electrons by n-propanol. The measured values are indicated by red circles, the all-electron calculated values by thin blue lines, and the pseudopotential values by thick green lines.

matching between the near-forward cross section, which is dominated by dipolar scattering, and the cross section at intermediate and high angles, dominated by short-range interactions described by the SMC calculation, is achieved by varying ℓ_{max} with energy, where ℓ_{max} is the maximum partial wave retained from the half-expanded SMC amplitude $f(\vec{k}_{in}, \ell_{out}, m_{out})$ [6]. In the present work, we gradually increased ℓ_{max} from 2 at 1 eV to 10 at 50 eV. The values of ℓ_{max} used are consistent with the semiclassical criterion $\ell_{max} \sim pR$, where p is the momentum of the projectile electron and R the radial extent of the one-electron basis set. Specifically, in the pseudopotential calculation for propanol, we used $\ell_{max}=2$ at 1 eV and 2 eV, $\ell_{max}=5$ at 5 eV, $\ell_{max}=6$ at 10 eV, $\ell_{max}=7$ at 15 eV, $\ell_{max}=8$ at 20 and 30 eV, and $\ell_{max}=10$ at 50 and 100 eV, while for butanol, we used $\ell_{max}=2$ at 1 eV, $\ell_{max}=3$ at 2 and 3 eV, $\ell_{max}=5$ at 5 eV, $\ell_{max}=6$ at 10 eV, $\ell_{max}=7$ at 15 eV, $\ell_{max}=9$ at 20 and 30 eV, and $\ell_{max}=10$ at 50 and 100 eV. Similarly, the all-electron calculations for propanol used $\ell_{max}=2$ from 1 to 2 eV, 3 from 2.5 to 4.5 eV, 4 at 5 and 5.5 eV, 5 from 6 to 10 eV, 6 from 11 to 15 eV, 7 at 20 eV, 8 at 30 eV, and 10 at 40 and 50 eV, while those for butanol used $\ell_{max}=2$ at 1 and 1.5 eV, 3 from 2 to 3 eV, 4 from 3.5 to 4.5 eV, 5 from 5 to 8 eV, 6 from 9 to 12 eV, 7 from 13 to 15 eV, 8 at 20 eV, 9 at 30 eV, and 10 at 40 and 50 eV.

III. RESULTS AND DISCUSSION

The present measured and calculated DCSs for elastic scattering of electrons by n-propanol are shown in Fig. 1 from 1 to 50 eV, and the experimental values are listed in Table II up to 100 eV. Despite differences in detail, there is

TABLE II. Measured differential cross section (10^{-16} cm^2/sr) for elastic electron scattering by *n*-propanol. The second column at each energy lists the error estimate. Italicized entries are extrapolated values used in computing the integral elastic (σ_I) and momentum-transfer (σ_{MT}) cross sections, which are listed, along with their error estimates, at the foot of the columns. The notation $[n]$ signifies $\times 10^n$.

Angle (deg)	1 eV		2 eV		5 eV		10 eV		15 eV		20 eV		30 eV		50 eV		100 eV	
0	*3.72[6]*		*7.44[6]*		*1.00[5]*		*2.50[4]*		*2.00[3]*		*1.00[3]*		*3.00[3]*		*500.0*		*1.00[3]*	
5	*353.0*		*177.0*		*150.0*		*80.0*		*70.0*		*180.0*		*200.0*		105.0	14.0	113.0	14.0
10	*88.5*		*44.3*		*57.0*		39.0	5.5	35.8	5.0	49.5	6.7	64.9	8.1	52.6	6.8	35.7	4.2
15	*39.5*		22.9	3.1	22.1	2.2	27.8	3.2	26.4	3.8	*27.0*		*32.0*		*18.0*		*10.3*	
20	20.5	3.0	12.1	2.3	14.8	1.6	20.0	2.5	19.3	2.5	17.4	2.3	16.8	1.8	7.27	0.87	3.35	0.40
30	10.2	1.1	6.26	1.03	6.81	0.88	9.33	0.85	8.78	1.28	5.18	0.69	4.03	0.39	1.94	0.24	1.30	0.16
40	5.85	0.50	4.02	0.41	4.04	0.40	4.53	0.42	4.40	0.64	2.66	0.36	2.30	0.27	1.24	0.17	0.647	0.075
50	3.39	0.37	2.91	0.24	3.23	0.33	3.14	0.33	3.06	0.48	2.18	0.28	1.68	0.20	0.757	0.097	0.412	0.052
70	2.08	0.19	2.99	0.41	2.67	0.29	2.38	0.28	2.19	0.35	1.21	0.15	0.744	0.102	0.343	0.044	0.174	0.021
90	2.09	0.22	2.52	0.31	1.73	0.23	1.85	0.23	1.78	0.30	0.849	0.109	0.516	0.070	0.232	0.027	0.106	0.016
110	2.42	0.27	1.89	0.28	1.74	0.23	2.04	0.26	2.01	0.30	0.944	0.123	0.567	0.074	0.260	0.033	0.149	0.022
130	2.89	0.33	1.60	0.16	2.20	0.26	2.53	0.27	2.21	0.33	1.19	0.16	0.855	0.095	0.446	0.057	0.222	0.034
140	*2.89*		*1.6*		*2.45*		*2.7*		*2.5*		*1.4*		*1.1*		*0.5*		*0.3*	
150	*3.0*		*1.7*		*2.8*		*3.0*		*2.7*		*1.8*		*1.4*		*0.7*		*0.37*	
160	*3.2*		*1.9*		*3.2*		*3.4*		*3.0*		*2.2*		*2.0*		*0.9*		*0.5*	
170	*3.3*		*2.05*		*3.5*		*3.8*		*3.4*		*2.8*		*2.5*		*1.3*		*0.7*	
180	*3.4*		*2.2*		*3.7*		*4.3*		*3.8*		*3.5*		*3.3*		*1.8*		*1.0*	
σ_I	109.0	17.0	67.6	11.1	52.2	7.2	51.6	6.9	48.3	8.7	41.5	6.5	39.3	5.6	21.4	3.2	15.3	2.4
σ_{MT}	34.5	5.7	27.1	4.4	29.6	4.1	32.1	4.3	29.8	5.4	17.3	2.7	12.7	1.8	6.13	0.92	3.30	0.52

good overall agreement among the three sets of results. The two calculations, in particular, yield very similar DCSs, with the largest differences occurring at 1 eV. There are somewhat larger differences between the experimental DCSs and the calculations at most energies, though the qualitative agreement is very good.

Similar remarks apply to the DCSs for *n*-butanol shown in Fig. 2 and tabulated in Table III. However, in this case the two calculations show more marked differences at low energies and intermediate to high angles.

In both molecules, the ratio of the calculated to the measured DCSs at intermediate angles tends to increase with increasing energy. The calculated cross sections are smaller than the measurements at 5 eV, comparable at 10 eV, and larger at higher energies, though propanol at 15 eV is an exception to this trend. Our recent experience in studies of various molecules suggests that calculations of the present type, in which electronic-excitation and ionization channels are treated as closed, tend to overestimate the DCSs at intermediate scattering angles for higher collision energies, where the cross sections of those inelastic channels are significant. This effect probably explains the calculated DCSs being larger than experiment for intermediate angles and higher energies in both *n*-propanol and *n*-butanol. Indeed, recent studies of elastic electron-atom and electron-molecule scattering at intermediate energies by other researchers have shown that the inclusion of an absorbing potential to represent open inelastic channels decreases the elastic DCSs at intermediate angles and thereby improves agreement with experiment [31–35].

At the lowest energies, the calculated results are sensitive to both the treatment of polarization and the Born-dipole correction. As mentioned in Sec. II B, the all-electron calculations employ a larger set of CSFs in the polarization space, but employ only singlet-coupled excitations, while the pseudopotential calculations include CSFs built from both singlet- and triplet-coupled excitations. Moreover, the calculations differ in their one-electron basis sets and in the accuracy of the quadrature used to evaluate the free-electron Green's function, whose off-shell component is most impor-
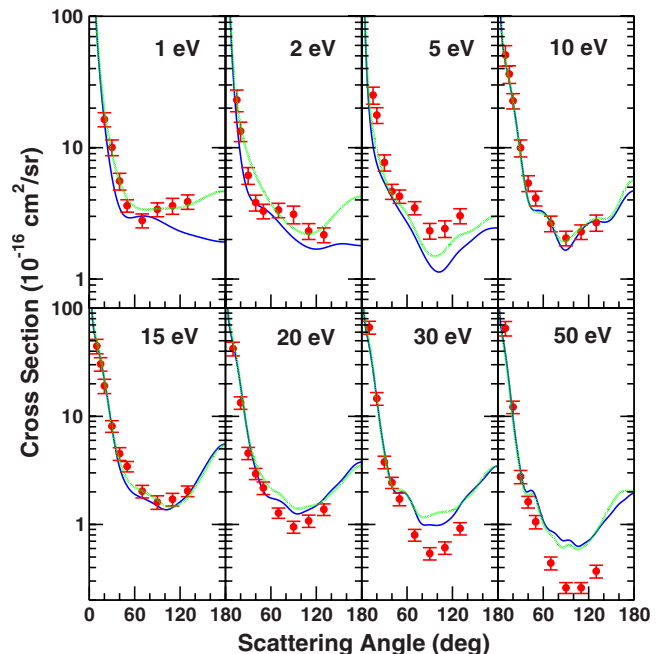

FIG. 2. (Color online) As in Fig. 1, for *n*-butanol.

tant at low energy. Sensitivity to these factors likely accounts for the larger differences between the two calculations, and between calculation and experiment, at 1 and 2 eV. At 1 eV, the pseudopotential DCS for butanol shows a backward peak and is thus in better agreement with experiment than is the all-electron DCS; at 2 eV, however, the all-electron result appears to describe better the shape of the measured DCS, including the absence of a backward peak and the presence of a shoulder. Though triplet virtual excitations mediated by the short-range exchange interaction could play a role at high scattering angles, the discrepancies between the pseudopotential and all-electron results cannot be unambiguously assigned to this aspect only; it is thus unclear which calculation, if either, is doing a better job at these energies. However, the good overall agreement between the two calculations at higher energies indicates that each treats polarization effects adequately there. In particular, neither the use of fewer CSFs in the pseudopotential calculations nor the neglect of triplet-coupled virtual excitations in the all-electron calculations appears to have much effect on the results at 5 eV and higher. This observation is consistent with the presence of a strong dipole potential that overwhelms the polarization (charge-induced-dipole) potential at large distances and therefore diminishes the importance of including target polarization effects. In water, another strongly polar system, the cross section has likewise been found to be insensitive to polarization effects (see, e.g., Refs. [36,37]).

At 10 eV, the calculated DCSs agree closely with each other and are considerably more structured than at lower or higher energies, displaying an angular pattern characteristic of f-wave resonances [38]. Although the experimental DCS was not taken at enough angles to verify this structure, at most measured angles it does agree quantitatively with the calculations. As shown in Fig. 3, the 10-eV DCS of the smallest alcohol, methanol, displays no such structure, but in ethanol it is weakly visible. Interestingly, similar f-wave structure is seen in the DCS of the alkanes ethane [39–42], n-propane [43,44], and n-butane [45,46], which differ from ethanol, n-propanol, and n-butanol only by substitution of an H atom for the OH group (but not seen in methane [40,47]). In the alkanes, however, the structure is more pronounced at lower energies ($\sim$6–8.5 eV) than it is at 10 eV. The same energy dependence holds for ethanol [6,48], but as seen in Fig. 4, the energy dependence in the larger alcohols is different, with the f-wave structure being most marked at 10 eV and progressively weakening as the energy decreases to 6 eV. This may indicate that our treatment of polarization in n-propanol and n-butanol is not fully converged, leading to resonances being placed too high in energy; however, given the excellent agreement between the two calculations, which used different polarization treatments, it may also reflect a true destabilization of the resonances in these larger alcohols.

In the alkanes, the f-wave behavior of the DCS appears to be associated with a broad peak in the integral cross section (ICS) that is also seen in the methane ICS and frequently interpreted as due to C-H and/or C-C σ^* shape resonances. Indeed, the cross sections for electron-impact excitation of C-H stretching vibrations in methane [49–52], ethane [53,54], propane [43,55], methanol [56], and ethanol [3] show broad peaks near 7.5 eV indicative of C-H σ^* reso-
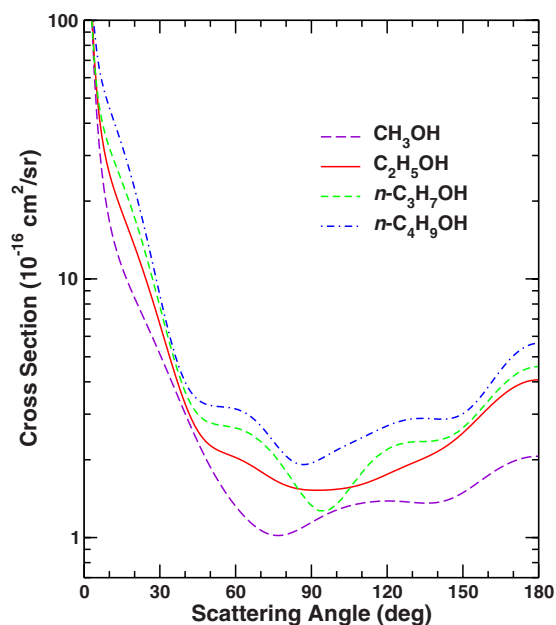

FIG. 3. (Color online) Calculated (pseudopotential) differential cross sections for elastic electron scattering by methanol, ethanol, n-propanol, and n-butanol at 10 eV impact energy. Methanol and ethanol results are from Ref. [6].

nances, while similar broad enhancements in the excitation cross sections for bending and C-C stretching modes of ethane [53,54] and propane [43,55] suggest the simultaneous presence of C-C σ^* resonances. For ethane, these observations are neatly rationalized by the near degeneracy of the two lowest valence virtual orbitals, $2e_u$ (C-H σ^*) and $3a_{2u}$ (C-C σ^*) [41,53,54]. A minimal-basis-set Hartree-Fock calculation shows that the lowest virtual orbitals of propane are likewise closely spaced and of both C-H and C-C σ^* character. In the alcohols, C-O and O-H σ^* resonances may also be present. The condensed-phase electron-impact spectra of methanol measured by Wen et al. [56] do in fact show broad peaks centered near 6 eV for excitation of both the C-O and
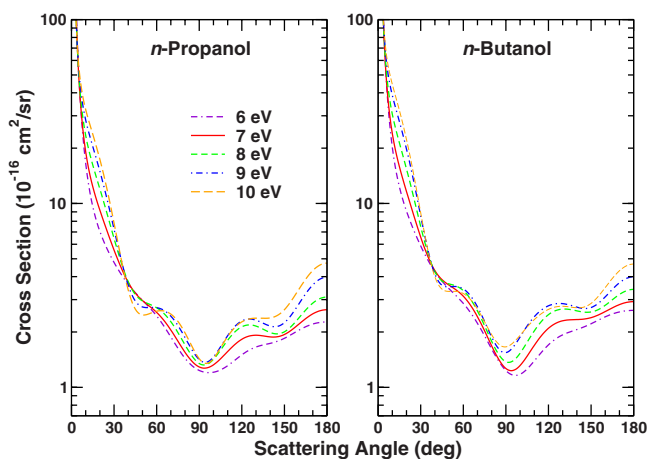

FIG. 4. (Color online) Calculated (all-electron) differential cross sections for elastic electron scattering by n-propanol (left) and n-butanol (right), showing the evolution of the angular structure from 6 to 10 eV collision energy.

O-H stretching modes, although they conclude the O-H σ^* resonance is actually centered near 4 eV. Ibănescu *et al.* [3] also place the O-H σ^* resonance at low energy, associating it with the sudden onset at the thermodynamic threshold ($\approx$3 eV) of CH_3O^- in the dissociative-attachment (DA) spectrum of methanol and of $C_2H_5O^-$ in the DA spectrum of ethanol, as well as with an excitation spectrum for the O-H stretching mode of ethanol that peaks below 1 eV. In minimal-basis-set Hartree-Fock calculations on the alcohols, we consistently find the lowest virtual orbital to be of mixed C-O and O-H σ^* character and to lie considerably ($\sim$3 eV) lower than the first virtual orbital of the alkanes, computed in the same basis set. On the other hand, the other low-energy minimal-basis virtual orbitals, though mostly of C-C and C-H σ^* character, do in some cases have C-O and O-H σ^* admixtures. Likewise, if we form energy pseudoeigenstates in the square-integrable many-particle basis set used for the scattering calculation, we find some single-particle states in the $6-12$ eV range that have density on the hydroxyl moiety. Thus states of at least partial C-O or O-H σ^* shape-resonant character in this energy range cannot be ruled out. In sum, overlapping resonances of various characters appear to give rise to the broad peak in the ICS of the alkanes and alcohols; however, the *f*-wave pattern in the DCS, present in both alkanes and alcohols, but absent in methane and methanol, might have a specific connection to C-C σ^* resonances.

Extracting an ICS for *n*-propanol or *n*-butanol from either the measured or calculated DCS is problematic. In polar molecules such as these, the ICS includes a large contribution from the extreme forward angles that cannot be reliably estimated by extrapolation of our measurements or obtained from our SMC calculations, and that therefore can be included in either only via the dipole-Born correction. Moreover, the magnitude of that contribution is sensitive to the rotational energy loss; the ICS is thus temperature dependent and should, strictly, be evaluated for a thermal ensemble of rotational states using the appropriate transition energies and moments [57]. With these caveats, we present ICS values in Fig. 5 that incorporate dipole-Born contributions calculated for energy losses that are roughly appropriate for typical transitions at a temperature of 300 K: namely 1.7 and 1.3 meV for *n*-propanol and *n*-butanol, respectively. To give a notion of the importance of the forward peak, we note that scattering at angles $\leqslant$2° contributes over 40% of the calculated butanol ICS at 1 eV, about 15% at 10 eV, and 10% 30 eV. Momentum-transfer cross sections (MTCSs) may be calculated with much less ambiguity from our DCSs, because the $(1-\cos\theta)$ weighting makes the role of the forward peak less significant. Our results for the momentum transfer cross sections are presented in Fig. 6. The experimental MTCS and ICS values from 1 to 100 eV are also given in Tables II and III, along with the extrapolated DCS values used in the integrations. In some cases, the shape of the calculated DCSs was used as a guide in extrapolating the experimental DCSs to high angles.

The differences in the calculated ICS and MTCS values at low impact energies reflect differences in the high-angle DCSs, some of which are shown in Figs. 1 and 2. At higher energies, the calculated results agree well with each other and exhibit a broad maximum around 10 eV. As just dis-
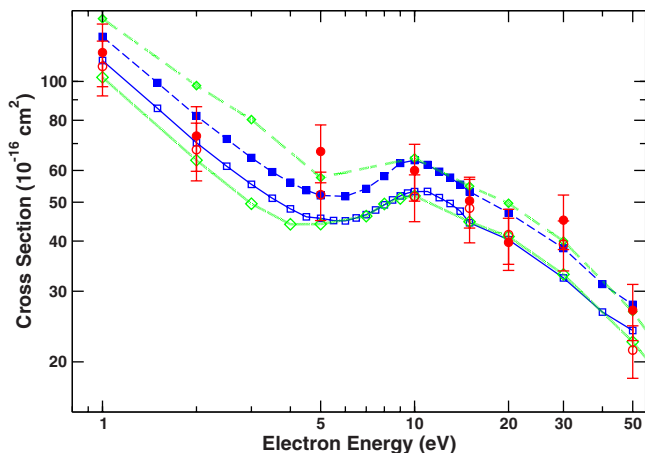

FIG. 5. (Color online) Integral elastic cross sections for electron collisions with *n*-propanol and *n*-butanol. Red circles are experimental values, thin blue lines with squares results from all-electron calculations, and thick green lines with diamonds results from pseudopotential calculations. Open symbols and solid lines are propanol data; solid symbols and dashed lines are butanol data. See text for discussion.

cussed, this maximum is likely due to multiple resonances, including those that give rise to the *f*-wave scattering pattern in the DCS; consistent with this picture, both the $^2A'$ and $^2A''$ symmetry components of our calculated ICSs (not shown) exhibit broad peaks between 8 and 12 eV. At most energies, the calculated and experimental ICSs agree within the error bars on the latter; however, agreement is less good for the MTCSs. The increasing tendency of the calculated MTCSs to exceed the experimental MTCSs above 15 eV likely reflects the overestimation of the intermediate-energy DCS due to lack of open inelastic channels in the calculations, as discussed above.
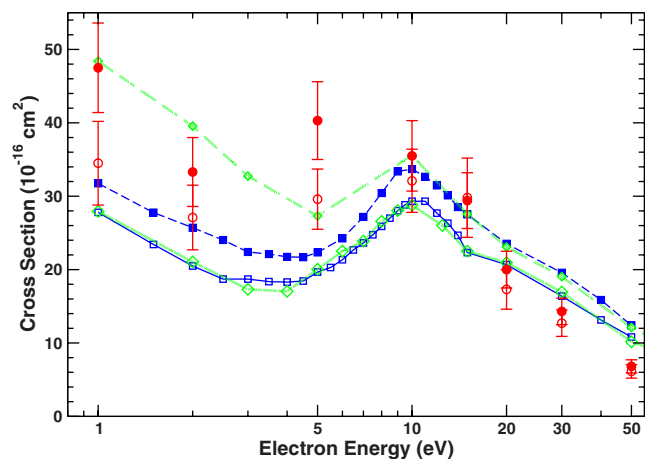

FIG. 6. (Color online) Momentum-transfer cross sections for electron collisions with *n*-propanol and *n*-butanol. Red circles are experimental values, thin blue lines with squares results from all-electron calculations, and thick green lines with diamonds results from pseudopotential calculations. Open symbols and solid lines are propanol data; solid symbols and dashed lines are butanol data.

TABLE III. Measured differential cross sections (10^{-16} cm^2/sr) for elastic electron scattering by n-butanol. The second column at each energy lists the error estimate. Italicized entries are extrapolated values used in computing the integral elastic (σ_I) and momentum-transfer (σ_{MT}) cross sections, which are listed, along with their error estimates, at the foot of the columns. The notation $[n]$ signifies $\times 10^n$.

Angle (deg)	1 eV		2 eV		5 eV		10 eV		15 eV		20 eV		30 eV		50 eV		100 eV	
0	*6.36[6]*		*1.27[7]*		*3.12[6]*		*6.36[4]*		*9.55[3]*		*4.00[3]*		*6.00[3]*		*1.20[3]*		*1.40[3]*	
5	*353.0*		*127.0*		*200.0*		*100.0*		*100.0*		*160.0*		107.0	15.4	114.0	18.8	106.0	13.0
10	*88.5*		*44.3*		*67.0*		50.7	9.0	44.7	6.9	42.3	6.1	66.6	9.1	65.3	10.0	28.8	4.0
15	*39.5*		23.1	4.3	25.1	3.7	36.4	5.6	30.5	4.3	*23.3*		*32.3*		*25.7*			
20	16.4	2.0	13.4	2.3	17.7	2.4	22.7	3.0	19.1	2.9	13.4	1.8	14.6	2.0	12.2	1.6	3.18	0.37
30	10.1	1.4	6.15	0.90	7.72	1.09	9.97	1.47	8.11	1.00	4.57	0.59	3.78	0.50	2.77	0.39	1.39	0.19
40	5.57	0.81	3.82	0.53	4.65	0.61	5.37	0.74	4.52	0.61	2.95	0.35	2.44	0.29	1.62	0.20	0.686	0.099
50	3.62	0.39	3.29	0.42	4.26	0.50	4.13	0.53	3.44	0.38	2.18	0.29	1.72	0.23	1.06	0.15	0.412	0.056
70	2.79	0.34	3.35	0.42	3.48	0.40	2.65	0.36	2.03	0.27	1.28	0.14	0.804	0.100	0.438	0.057	0.171	0.024
90	3.39	0.41	3.11	0.48	2.33	0.32	2.05	0.26	1.61	0.23	0.952	0.120	0.542	0.071	0.255	0.035	0.105	0.014
110	3.61	0.50	2.32	0.32	2.42	0.35	2.29	0.29	1.71	0.23	1.08	0.14	0.609	0.075	0.259	0.032	0.170	0.023
130	3.88	0.49	2.17	0.28	3.03	0.40	2.69	0.38	2.04	0.23	1.38	0.17	0.924	0.120	0.370	0.050	0.220	0.030
140	*3.9*		*2.1*		*3.5*		*2.9*		*2.5*		*1.8*		*1.3*		*0.5*		*0.32*	
150	*4.2*		*2.25*		*4.0*		*3.2*		*2.9*		*2.3*		*1.8*		*0.8*		*0.45*	
160	*4.4*		*2.4*		*4.4*		*3.7*		*3.9*		*2.9*		*2.4*		*1.0*		*0.6*	
170	*4.5*		*2.7*		*4.7*		*4.2*		*4.3*		*3.5*		*3.0*		*1.5*		*0.9*	
180	*4.6*		*3.0*		*4.9*		*4.7*		*4.8*		*4.7*		*4.0*		*2.0*		*1.2*	
σ_I	118.0	21.0	73.1	13.4	66.9	11.0	60.0	9.7	50.4	7.3	39.7	5.9	45.1	7.0	26.9	4.3	14.4	2.3
σ_{MT}	47.5	6.1	33.3	4.7	40.3	5.3	35.5	4.8	29.4	3.8	20.0	2.5	14.3	1.8	6.81	0.90	3.61	0.49

IV. CONCLUSION

We have presented experimental and theoretical differential cross sections for elastic scattering of low-energy electrons by two primary straight-chain alcohols, n-propanol and n-butanol. To our knowledge, these are the first such measurements and calculations for either molecule. In the forward direction, the cross sections exhibit the strong peak characteristic of polar molecules; at higher angles, an f-wave pattern is visible around 10 eV. Clear patterns of similarity emerge on comparison with the smaller alcohols, methanol and ethanol, and with the straight-chain alkanes.

ACKNOWLEDGMENTS

[1] T. Skalický and M. Allan, J. Phys. B **37**, 4849 (2004).

[2] V. S. Prabhudesai, A. H. Kelkar, D. Nandi, and E. Krishnakumar, Phys. Rev. Lett. **95**, 143202 (2005).

[3] B. C. Ibănescu, O. May, A. Monney, and M. Allan, Phys. Chem. Chem. Phys. **9**, 3163 (2007).

[4] M. Orzol, I. Martin, J. Kocisek, I. Dabkowska, J. Langer, and E. Illenberger, Phys. Chem. Chem. Phys. **9**, 3424 (2007).

[5] D. Bouchiha, J. D. Gorfinkiel, L. G. Caron, and L. Sanche, J. Phys. B **40**, 1259 (2007).

[6] M. A. Khakoo, J. Blumer, K. Keane, C. Campbell, H. Silva, M. C. A. Lopes, C. Winstead, V. McKoy, R. F. da Costa, L. G. Ferreira, M. A. P. Lima, and M. H. F. Bettega, Phys. Rev. A **77**, 042705 (2008).

[7] D. Antoni, V. V. Zverlov, and W. H. Schwarz, Appl. Microbiol.

Biotechnol. **77**, 23 (2007).

[8] M. A. Khakoo, K. Keane, C. Campbell, N. Guzman, and K. Hazlett, J. Phys. B **40**, 3601 (2007).

[9] C. Winstead and V. McKoy, Comput. Phys. Commun. **128**, 386 (2000).

[10] M. H. F. Bettega, L. G. Ferreira, and M. A. P. Lima, Phys. Rev. A **47**, 1111 (1993).

[11] K. Takatsuka and V. McKoy, Phys. Rev. A **24**, 2473 (1981).

[12] K. Takatsuka and V. McKoy, Phys. Rev. A **30**, 1734 (1984).

[13] N. Đurić, I. Čadež, and M. Kurepa, Fizika (Zagreb) **21**, 339 (1989).

[14] R. Rejoub, C. D. Morton, B. G. Lindsay, and R. F. Stebbings, J. Chem. Phys. **118**, 1756 (2003).

[15] J. E. Hudson, M. L. Hamilton, C. Vallance, and P. W. Harland, Phys. Chem. Chem. Phys. **5**, 3162 (2003).

[16] A. N. Zavilopulo, F. F. Chipev, and L. M. Kokhtych, Nucl. Instrum. Methods Phys. Res. B **233**, 302 (2005).

[17] M. Hughes, K. E. James, Jr., J. G. Childers, and M. A. Khakoo, Meas. Sci. Technol. **14**, 841 (2003).

[18] J. H. Brunt, G. C. King, and F. H. Read, J. Phys. B **10**, 1289 (1977).

[19] R. K. Nesbet, Phys. Rev. A **20**, 58 (1979).

[20] D. F. Register, S. Trajmar, and S. K. Srivastava, Phys. Rev. A **21**, 1134 (1980).

[21] M. W. Schmidt, K. K. Baldridge, J. A. Boatz, S. T. Elbert, M. S. Gordon, J. H. Jensen, S. Koseki, N. Matsunaga, K. A. Nguyen, S. J. Su, T. L. Windus, M. Dupuis, and J. A. Montgomery, J. Comput. Chem. **14**, 1347 (1993).

[22] A. Maeda, F. C. De Lucia, E. Herbst, J. C. Pearson, J. Riccobono, E. Trosell, and R. K. Bohn, Astrophys. J., Suppl. Ser. **162**, 428 (2006), and references therein.

[23] T. N. Wassermann, P. Zielke, J. J. Lee, C. Cézard, and M. A. Suhm, J. Phys. Chem. A **111**, 7437 (2007).

[24] S. Höfener, F. A. Bischoff, A. Glöß, and W. Klopper, Phys. Chem. Chem. Phys. **10**, 3390 (2008).

[25] *CRC Handbook of Chemistry and Physics*, 79th ed., edited by D. R. Lide (CRC Press, Boca Raton, 1998).

[26] C. W. Bauschlicher, Jr., J. Chem. Phys. **72**, 880 (1980).

[27] M. H. F. Bettega, A. P. P. Natalense, M. A. P. Lima, and L. G. Ferreira, Int. J. Quantum Chem. **60**, 821 (1996).

[28] T. H. Dunning, Jr., J. Chem. Phys. **53**, 2823 (1970).

[29] G. B. Bachelet, D. R. Hamann, and M. Schlüter, Phys. Rev. B **26**, 4199 (1982).

[30] C. Winstead, V. McKoy, and M. H. F. Bettega, Phys. Rev. A **72**, 042721 (2005).

[31] L. M. Brescansin, P. Rawat, I. Iga, M. G. P. Homem, M.-T. Lee, and L. E. Machado, J. Phys. B **37**, 471 (2004).

[32] H. Cho, R. P. McEachran, H. Tanaka, and S. J. Buckman, J.

Phys. B **37**, 4639 (2004).

[33] H. Cho, R. P. McEachran, S. J. Buckman, D. M. Filipović, V. Pejčev, B. P. Marinković, A. D. Stauffer, and E. J. Jung, J. Phys. B **39**, 3781 (2006).

[34] H. Cho, Y. S. Park, E. A. y Castro, G. L. C. de Souza, I. Iga, L. E. Machado, L. M. Brescansin, and M.-T. Lee, J. Phys. B **41**, 045203 (2008).

[35] L. M. Brescansin, L. E. Machado, M.-T. Lee, H. Cho, and Y. S. Park, J. Phys. B **41**, 185201 (2008).

[36] T. N. Rescigno and B. H. Lengsfield, Z. Phys. D: At., Mol. Clusters **24**, 117 (1992).

[37] R. Greer and D. Thompson, J. Phys. B **27**, 3533 (1994).

[38] F. H. Read, J. Phys. B **1**, 893 (1968).

[39] D. Matsunaga, M. Kubo, and H. Tanaka, in *Proceedings of the 12th International Conference on the Physics of Electronic and Atomic Collisions*, edited by S. Datz (North-Holland, Amsterdam, 1981), p. 358.

[40] P. J. Curry, W. R. Newell, and A. C. H. Smith, J. Phys. B **18**, 2303 (1985).

[41] H. Tanaka, L. Boesten, D. Matsunaga, and T. Kudo, J. Phys. B **21**, 1255 (1988).

[42] W. Sun, C. W. McCurdy, and B. H. Lengsfield III, J. Chem. Phys. **97**, 5480 (1992).

[43] L. Boesten, M. A. Dillon, H. Tanaka, M. Kimura, and H. Sato, J. Phys. B **27**, 1845 (1994).

[44] M. H. F. Bettega, R. F. da Costa, and M. A. P. Lima, Phys. Rev. A **77**, 052706 (2008).

[45] A. R. Lopes, M. H. F. Bettega, M. A. P. Lima, and L. G. Ferreira, J. Phys. B **37**, 997 (2004).

[46] M. H. F. Bettega, M. A. P. Lima, and L. G. Ferreira, J. Phys. B **40**, 3015 (2007).

[47] H. Tanaka, T. Okada, L. Boesten, T. Suzuki, T. Yamamoto, and M. Kubo, J. Phys. B **15**, 3305 (1982).

[48] C. Winstead and V. McKoy (unpublished results).

[49] H. Tanaka, M. Kubo, N. Onodera, and A. Suzuki, J. Phys. B **16**, 2861 (1983).

[50] L. Boesten and H. Tanaka, J. Phys. B **24**, 821 (1991).

[51] T. W. Shyn, J. Phys. B **24**, 5169 (1991).

[52] R. Čurík, P. Čársky, and M. Allan, J. Phys. B **41**, 115203 (2008).

[53] L. Boesten, H. Tanaka, M. Kubo, H. Sato, M. Kimura, M. A. Dillon, and D. Spence, J. Phys. B **23**, 1905 (1990).

[54] R. Merz and F. Linder, J. Phys. B **36**, 1143 (2003).

[55] R. Merz and F. Linder, J. Phys. B **36**, 2921 (2003).

[56] A. T. Wen, M. Michaud, and L. Sanche, Phys. Rev. A **54**, 4162 (1996).

[57] Y. Okamoto, K. Onda, and Y. Itikawa, J. Phys. B **26**, 745 (1993).